

Classifying Seabed Sediments Using the Local Auto-correlation Features

Yasuhiro Tan*, Joo Kooi Tan*, Hyungseop Kim*, Seiji Ishikawa*

* Mechanical and Control Engineering, Kyushu Institute of Technology

Abstract: Understanding the distribution of seafloor sediment using a side-scan sonar is very important to grasp the distribution of seabed resources. This task is traditionally carried out by a skilled human operator. However, with the appearance of Autonomous Underwater Vehicles, automated processing is now needed to tackle the large amount of data produced and to enable on the fly adaptation of the missions and near real time update of the operator. We propose in this paper a method that applies a higher-order local auto-correlation feature and a subspace method to the acoustic image provided by the side-scan sonar to classify seabed sediment automatically. In texture classification, the proposed method outperformed other methods such as a gray level co-occurrence matrix and a Local Binary Pattern operator. Experimental results show that the proposed method produces consistent maps of a seafloor.

Keywords Seafloor sediment, side-scan sonar, higher-order local auto-correlation features, texture classification.

1.Introduction

The ocean accounting for an area of approximately 70% on the earth is the property which is common to all creatures on the earth as well as a human. It is used for fish farming, land reclaiming, and so on. The resources such as oil and the natural gas methane hydrate manganese nodule are still unexploited in the bottom of the sea. They are called seabed resources. Nowadays, the use of those seabed resources is requested to a large extent according to the recent rapid technological development.

The information on the quality of the surface of a seabed is important to grasp the distribution of such seabed resources. The distribution map on the information is generally made using a bottom sampler which samples the surface of the seabed interested point by point, and these point-wise data are regarded as representing the seabed area under investigation. Obviously this investigation gives less exact information on the surface of a larger seabed area, even if the number of the sampling points increases. Since the light does not reach at most part under the surface level of the sea, it is necessary to

use acoustic energy there which has very good permeability irrespective of liquid, gas or solid.

A side scan sonar which is one of the seabed probes using the sound is a remote sensing apparatus and it brings the sound wave reflection image of the bottom of the sea in a short-term investigation. **Figure 1** summarizes the image generation with the side scan sonar. The side scan sonar irradiates a sound wave to the seabed and visualize the seabed topography in an image form by analyzing the reflected sound waves. It provides the surface information on a broad area of the seabed precisely as well as in a high speed.

However, geological study of the seabed surface employing the acoustic images largely depends on the knowledge and experience of an engineer and it is sometimes difficult to be objective.

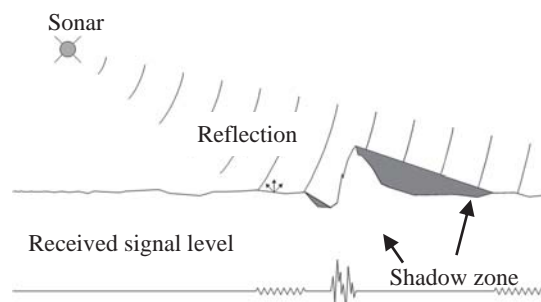


Fig. 1. Schematic of a side-scan sonar.

Sensuicho 1-1, Tobata, Kitakyushu,
Fukuoka 804-8550 Japan
Phone and Fax: +81-93-881-2189
e-mail: ytan@ss10.cntl.kyutech.ac.jp

There are some automated methods for analyzing the acoustic images of the seabed. Classification of the seabed soil from sound images of the side scan sonar employing texture analysis was performed by Yamamoto, et al. [1], but the result of the analysis was not evaluated using actual seabed soils. In recent years, Atallah and Smith [2] proposed a method of analyzing the seabed soils using both the sound image and the depth information provided by a depth sensor. But it is unsuitable for the classification in real time because of the acquisition of the depth information. For a practical use, the developed technique should give a simple procedure and high precision in the classification.

This paper proposes an automatic method of classifying the seabed soils from a sound image based on the HLAC (Higher-order Local Auto-Correlation) [3] feature. HLAC is a basic as well as general image feature directing attention to the co-occurrence nature of texture patterns. It has been employed for the recognition of a face [4, 5], a letter [6], gesture [7], etc. It has also been applied to medical image analysis, remote sensing image analysis, object detection and recognition based on the texture, and so on. We show the effectiveness of the proposed method by applying it to real seabed images. We also compare the proposed method with the method using a gray level co-occurrence matrix by Yamamoto, et al. [8] and a LBP (Local Binary Pattern) technique [9] used widely in texture analysis.

In the following, Section II explains the proposed method. Section III shows experimental results using the side scan sonar images of various kinds of seafloor topography. Section IV gives discussion. Section V concludes the paper with recommended directions for future work.

2. Classification of the seabed

Sonic waves are beamed toward the surface of the seabed, and the difference in the sound waves' reflection intensity is displayed as different shadings to express the seabed by an image. In the course of sound wave propagation through seawater, acoustic energy is attenuated by being changed to other forms of energy. This is called absorption loss [10]. The amount of attenuation of sound waves Np (dB) is defined by the following formula;

$$Np = 20 \log r + \alpha r$$

$$\alpha = 0.22f + 0.000175f^2 \quad (1)$$

Here r is the distance from the sound source to the object (km) and α is the coefficient depending on the frequency of the sound wave f .

A. Flow of the proposed method

The proposed method makes a feature space from training data which are sound images of the seabed. An unknown sound image of the seabed is classified into one of the several classes representing seabed sediments using the feature space. The HLAC feature which extracts co-occurrence of texture is employed for describing the texture of seabed sediments. The subspace method is employed to make the feature space and to perform the classification. The schematic diagram of the classification is given in **Figure 2**.

The HLAC feature vectors are computed, in advance, from training image data of all seabed sediments. Then, the Principal Component Analysis (PCA) is applied to the vectors to compress the dimension and to form a subspace. Given an unknown sound image, the HLAC feature vector is calculated from every scanned window on the image and the distance of the vector with each subspace is evaluated for classification. The vector, i.e., the unknown sound image is classified into the class with which the distance is the minimum.

B. Extraction of the features

The proposed method uses the HLAC features to extract texture features. If the gray value of the target image at the point r is denoted by $f(r)$, the N th autocorrelation function is defined by the following equation;

$$x(a_1, a_2, \dots, a_N) = \int f(r)f(r+a_1) \cdots f(r+a_N)dr \quad (2)$$

The HLAC feature is a basic image feature based on this function. Since the local correlation between nearby

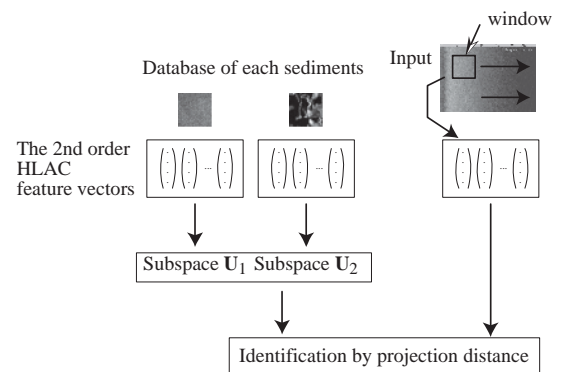


Fig. 2. Flowchart of the classification.

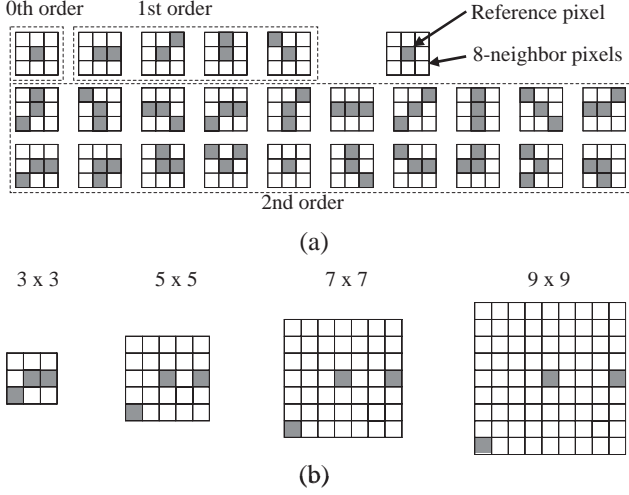


Fig. 3. 25 local patterns for calculating HLAC features: (a) Local 3x3 masks up to the second order, (b) Used 4 sizes of the mask patterns.

pixels is more important in an image data, we set $N=2$ and consider the domain of local 3x3 pixels around the reference point r , that is, the correlation up to three points in the local domain is taken into account. Then the HLAC feature performs the calculation using 25 mask patterns of 3x3 pixels (1 zero-dimensional, 4 one-dimensional and 20 two-dimensional patterns) as shown in **Figure 3(a)**. As one mask pattern produces a single value from a window, a feature vector is defined by a 25-dimensional vector. The 0th order, the 1st order and the 2nd order HLAC features are calculated by the following equations, respectively;

$$\begin{aligned} x(a_0) &= \int f(r) dr \\ x(a_1) &= \int f(r) f(r+a_1) dr \\ x(a_2) &= \int f(r) f(r+a_1) f(r+a_2) dr \end{aligned} \quad (3)$$

The calculation of the HLAC feature is to multiply the gray values corresponding to the dark pixels of each mask pattern and to sum them in the window interested.

In the present research, masks of the size 3x3, 5x5, 7x7 and 9x9 are also employed as shown in **Figure 3(b)** in order to extract texture features of larger domains. Note that the mask of each size has 25 patterns similar to the mask of 3x3. Therefore the dimension of the actual feature vector is 100. These mask patterns with larger sizes extract lower frequency features compared to the 3x3 mask, as they calculate the correlation among two or three mutually distant pixels. This is equivalent to applying a 3x3 mask pattern to a lower resolution image made

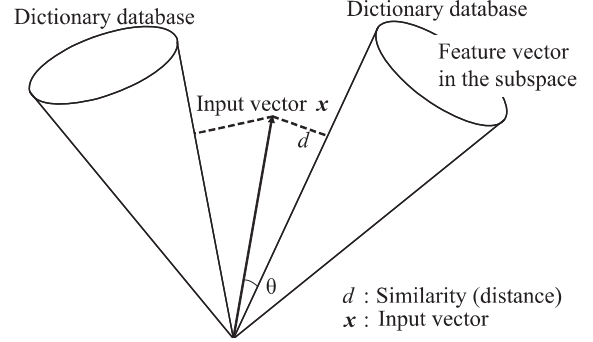


Fig. 4. Schematic of the subspace method.

by reducing pixels of the original image in a pyramidal way. The 3x3 mask pattern extracts high-frequency component of the image. By considering variation in the mask sizes, low frequency feature as well as high frequency feature can be extracted, which may be advantageous to the seabed soil analysis.

C. Recognition by the subspace method

Figure 4 shows the concept of the subspace method [11]. The subspace method is a method of class discrimination. The proposed method classifies the seabed sediments by the subspace method, in which each class of the seabed sediment has its own subspace and an unknown image is classified into one of those subspaces by a distance measure. Each class is learning the subspace of low-dimensional representation of the class. By determining the unknown patterns are to be approximated best in each subspace, to identify the class of unknown pattern.

Given N learning images of a sediment, the HLAC feature vectors x_i ($i=1,2,\dots,N$) are calculated from them. The covariance matrix C defined by Eq.(4) is calculated using the feature vectors. Here μ is an average vector of x_i .

$$C = \frac{1}{N} \sum_{i=1}^N (x_i - \mu)(x_i - \mu)^T \quad (4)$$

Eigenvalues λ_i and corresponding eigenvectors u_i are calculated from the covariance matrix. We arrange the eigenvalues in the descending order. Compression of the feature space is done using the accumulated contribution ratio η_K ($K \leq N$) defined by

$$\eta_K = \frac{\sum_{i=1}^K \lambda_i}{\sum_{i=1}^N \lambda_i} \quad (5)$$

Here N is the number of dimension. We choose K eigenvectors $\mathbf{u}_1, \dots, \mathbf{u}_K$, where K is the minimum value satisfying $\eta_K > \mu$. Here μ is a threshold determined experimentally. These K eigenvalues make a subspace.

If we denote $\mathbf{U}_K = (\mathbf{u}_1, \dots, \mathbf{u}_K)$, the projection matrix is expressed as $\mathbf{U}_K \mathbf{U}_K^T$. Then the distance d between an unknown feature vector \mathbf{x} and the subspace defined by \mathbf{U}_K is given by

$$d = \mathbf{x}^T \mathbf{x} - \mathbf{x}^T \mathbf{U}_K \mathbf{U}_K^T \mathbf{x}. \quad (6)$$

The value d is the index for the classification in the proposed method.

If there are M kinds of seabed sediments, we define M subspaces. Given an unknown vector, the distances d_m to a sediment class m ($m=1,2,\dots,M$) are examined to find the minimum value. In case the unknown vector does not belong to any class, it is rejected. The rejection occurs if the minimum distance exceeds a certain threshold, or the following inequality holds with respect to any m and a given threshold θ ;

$$\min_K \left\{ \frac{\mathbf{x}^T \mathbf{U}_{m,K} \mathbf{U}_{m,K}^T \mathbf{x}}{\mathbf{x}^T \mathbf{x}} \right\} > \theta. \quad (7)$$

where $\mathbf{U}_{m,K}$ defines the subspace of the sediment class m and \mathbf{x} is an unknown vector.

3. Experimental results

A. Experimental setup

For the experiments, we used side-scan sonar images obtained in actual environments. Two sites were used for exploration; a muddy seabed and a sandy seabed. After lowering the sonar device into the water from the stern of the research vessel, we explored the area about 2000 meters wide and 2,000 meters long, and obtained sound images of the seabed. The water within the scope of the exploration was about 40 meters deep. The area was in

Table 1. Specifications of the sonar

Basic performance	
Frequency	340 kHz
Horizontal beamwidth	0.9 deg
Vertical beamwidth	60 deg
Range resolution	10 cm
Max operating depth	100 m
Max cable length	200+ m
Materials	Stainless steel, PVC and Polyurethane

spected by adjusting the sonar's towing depth to a set interval of 15 meters from the sea surface. The total navigation time was approximately 8 hours. **Table 1** shows the specifications of the used side-scan sonar. The acoustic reflectance is decided by the quality of the bottom of the range scanned by a side scan sonar.

The rock and the gravel reflectance is higher than sand and mud, and is bright on the side scan sonar record. Furthermore, the shape of the individual components of such materials has a large influence on the reflectance and strength of backscattering. Similarly, the seafloor topography is a factor to decide acoustic reflectance. Assuming that the terrain the sonar unit is facing is a plane view, if an incidence angle of the irradiated sound to a plane seabed becomes larger, the reflected sound wave becomes brighter on the record. On the contrary, return values become extremely weak when the incidence angle becomes smaller than 45 degrees. Therefore we limit the angle of the sound wave irradiation by a side scan sonar up to 45 degrees in this study. **Figure 5** shows change of the signal strength by the acoustic irradiation degree.

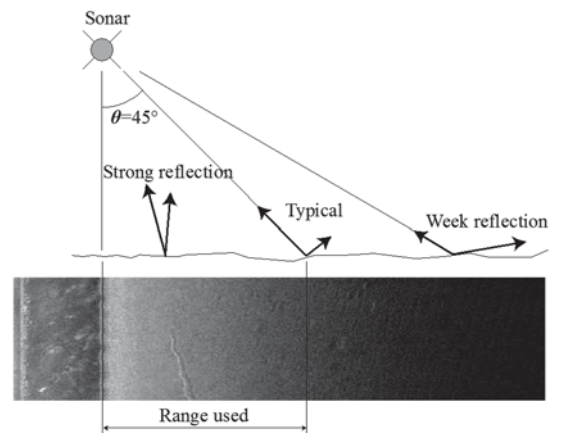


Fig. 5. The reflection intensity by irradiation angle.

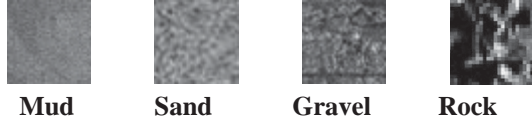


Fig. 6. Categories of seabed sediment images

B. Result of classification

In this study, we performed classification of four kinds of representative sediments, namely mud, sand, gravel and rock from the sound images of the side scan sonar obtained from a real seabed environment. In addition, we examined the relationship of classification rate and the size of the window for the HLAC features calculation on the image. Examples of the seabed sediments are shown in **Figure 6**. We separated a classification domain into four types of mesh regions (each having 12x12, 24x24, 36x36, 48x48 pixels) and calculated the feature vector at each region to classify it. The classification rate is defined by the following;

$$\text{Classification rate} = \frac{\text{Correctly classified regions}}{\text{All the divided regions}} \quad (8)$$

We prepared for 100 images with each of the four sizes of windows (12x12, 24x24, 36x36, 48x48 pixels) of four kinds of sediments (the mud, sand, gravel and rock) to make an image database. The prepared images therefore amounts to 1,600. The computer used for the calculation has 4 GB memory and a 2.66 GHz Intel Core 2 Duo processor. **Table 2** shows the classification rate with each sediment in relation to the size of the mesh region. As shown in the table, the sand region gave the highest classification rate, 90.2%. This may be because the sand region spreads uniformly and it gives high reflectance of the acoustic wave, resulting in a high contrast ultrasound images. The low classification rate of gravel and rock regions may come from the fact that gravels and rocks often exist on a sand and those regions do not always contain only gravels or rocks. The result of the classification with respect to the dimension of the subspace is as well given in **Figure 7**. The mesh region with 36x36 pixels achieved the highest classification rate.

Figure 8 shows the overall classification result of the seabed sound image by the proposed method. The very fine mud region of the grain form is shown by green. The sand region is yellow, the gravel region is red and the rock region is shown with blue. Under the investigation

ship, as the transmission pulse from a side scan sonar is emitted almost vertically to the seabed, the shadow of the sound wave is hard to be made, and there occurs a blank part called a water column. It is a blank area of both sides of the black line in **Figure 8**. Other blank areas are those where acquisition of seabed images is difficult because of weak reflection intensity of the sound wave. This water column part is a seawater part between the main body of the sonar and the bottom of the sea, and the seabed sediments cannot be classified. On the other hand, we were able to classify the domains where the reflection strength was relatively weak because of smaller (less than 45 degrees) incidence angles of the sound wave.

Although misclassification occurred sometimes, we judge that the result approached well the classification by the sea chart based on a geological background, because the classified regions distribute uniformly as well as continuously.

Table 2. Relation of the classification rate with each seabed sediment and the size of the mesh region along with the value K giving the maximum classification rate.

	[%]			
	12 x 12	24 x 24	36 x 36	48 x 48 pixels
Subspace dimension K	15	17	25	24
Mud region	54.4	71.3	76.1	76.9
Sand region	59.9	78.7	90.2	88.2
Gravel region	41.6	51.9	52.7	53.9
Rock region	39.5	40.7	42.3	40.6
Average rate	48.9	60.7	65.3	64.9

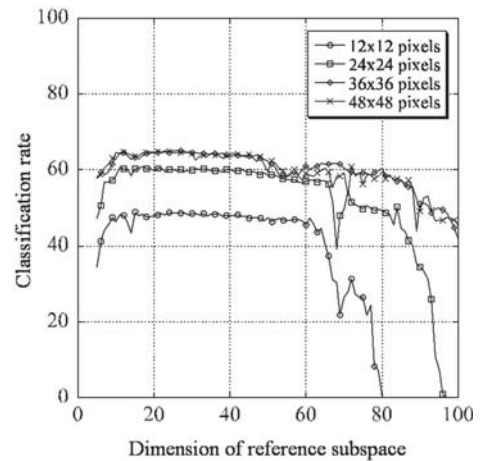


Fig. 7. Results of the classification. The abscissa is the dimension of the subspaces and the ordinate is the classification rate. A graph is shown with every size of the mesh region.

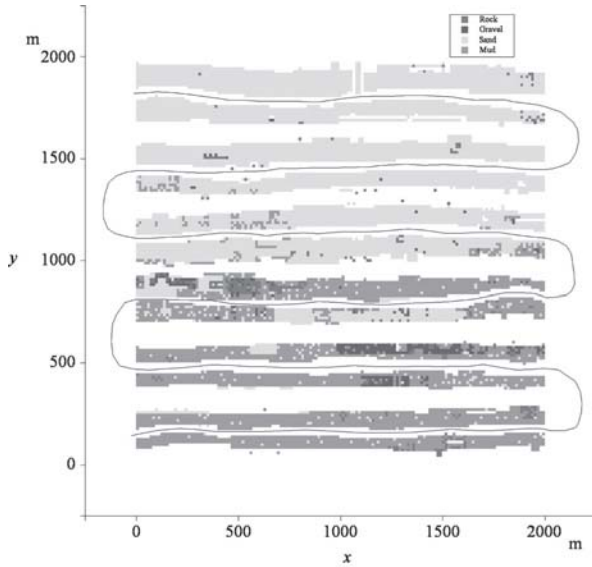


Fig. 8. Visual display of the result of the classification: The mud region is shown by green, the sand region yellow, the gravel region red and the rock region blue.

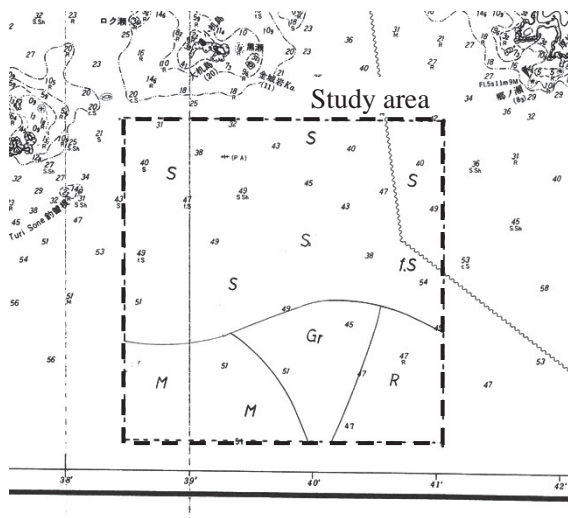


Fig. 9. Costal chart in the study area.

Table 3. Comparison of classification rate with other methods and proposed method

Identification technique	Classification rate
Higher-order Local AutoCorrelation	65.3
Gray Level Co-occurrence Matrix	57.6
Local binary patterns	31.2

4. Discussion

Although ground-truth data are necessary for determination of classification precision, it is actually difficult in the seabed sediments classification. Therefore we used the chart of the Japan Hydrographic Association (JHA) which classifies seabed sediments based on a geological background in order to evaluate the experimental results. **Figure 9** shows the chart by JHA of the study area.

As shown in **Figure 7**, the larger the mesh region is, the better the classification result is. This is because a smaller size of image reduces the amount of information. Since there is hardly difference between the case with 36x36 pixels and with 48x48 pixels, the most suitable domain is 36x36 pixels, in which case the best classification rate was 65.3%. Since the HLAC feature is an integral feature, a larger region may decrease difference of the HLAC feature among the set regions. Therefore, we consider that there is a region of the optimal size with the recognition area.

We performed some other kinds of texture feature extraction to evaluate the proposed method. We examined the feature of gray level co-occurrence matrix and the LBP used widely in texture analysis for the comparison with the HLAC feature. In the texture feature extraction by the gray level co-occurrence matrix, we used entropy, local homogeneity, moment, contrast at angles ($\theta=0, 45, 90, 135$) and distance ($d=1$). The LBP is a method of comparing the gray value of a pixel with its 8-neighbors and expresses large or small by 1 or 0 to make a 8-bit binary number. **Table 3** compares the classification rate in the entire study area between the proposed method and the other methods. The classification by LBP was the lowest and 31.2%. The reason for this may be that the LBP compresses the original image into a 256 level gradation image regardless of the actual gradation of the original, and the information on small shadow difference of mud and sand in the original image is lost by the normalization. **Table 3** shows that the proposed method achieved the best classification rate in comparison with two other methods.

The classification rate of 65.3% is not very high. It is, however, a reasonable result, if we consider that there is hardly clear borders among the seabed sediments. We may also add that, to the best of our knowledge, this is the first practical result on automatic seabed sediments classification. The fact that the classification rate

achieved about 90% with the sand region suggests further possible improvement of the proposed method.

There were not a few false-classification and false-reject between mud and sand, and sand and gravel. One of the main reasons for this misjudgment is that the sound images obtained from the border between mud and sand, for example, contained both of the sediments. Larger number of training images on the sediment borders may be necessary to solve this difficulty.

5. Conclusion

In this paper, we proposed a method of classifying seabed sediments using ultrasound images provided by a side scan sonar. The proposed method classifies the seabed sediments using Higher-order Local Auto-correlation feature and the subspace method. It has been confirmed throughout various experiments of texture classification that the HLAC feature is effective in classifying seabed sediments from their ultrasound images, though the classification precision depends on the size of a texture region. Since calculation of the HLAC feature is simple, high-speed operation is possible by hardware. From this fact, the proposed method is a highly practical and useful method.

In order to improve the precision of the classification, accumulation of sample data used as training data is necessary. Exact classification of the region on the border of the seabed sediments is also a future problem to be solved.

References

- [1] F. Yamamoto, T. Takeuchi, H. Tokuyama, K. Suehiro, A. Taira, "Classification of seafloor characteristics using IZANAGI side scan sonar imagery," *Transactions of Institute of Electronics, Information, and Communication Engineers*, Vol. 25, pp. 29-35, 1994.
- [2] Atallah, L., and P.J. Smith. "Automatic seabed classification by the analysis of sidescan sonar and bathymetric imagery," *IEEE Proceedings-Radar, Sonar and Navigation*, Vol. 151(5), pp.327-336, 2004.
- [3] N. Otsu, "Mathematical Studies on Feature Extraction in Pattern Recognition," (in Japanese) *Researches of the ETL*, Vol. 818, 1981.
- [4] Goudail, F., et al. "Face recognition system using local autocorrelations and multiscale integration," *Pattern Analysis and Machine Intelligence, IEEE Transactions on*, Vol. 18(10), pp. 1024-1028, 1996.
- [5] Kurita, T., N. Otsu, and T. Sato. "A face recognition method using higher order local autocorrelation and multivariate analysis," *Pattern Recognition*, 1992. Vol. II. Conference B: Pattern Recognition Methodology and Systems, Proceedings., 11th IAPR International Conference on. IEEE, pp. 213-216, 1992.
- [6] Cheng, H., et al. "Spam image discrimination using support vector machine based on higher-order local autocorrelation feature extraction," *Cybernetics and Intelligent Systems*, 2008 IEEE Conference on. IEEE, pp. 1017-1021, 2008.
- [7] Kurita, T., and Satoru H. "Gesture recognition using HLAC features of PARCOR images and HMM based recognizer," *Automatic Face and Gesture Recognition*, 1998. Proceedings. Third IEEE International Conference on. IEEE, pp. 422-427, 1998.
- [8] Peckinpah, S. H. "An improved method for computing gray-level cooccurrence matrix based texture measures," *CVGIP: Graphical Models and Image Processing*, Vol. 53(6), pp. 574-578, 1991.
- [9] Ojala, Timo, Matti Pietikainen, and Topi Maenpaa. "Multiresolution gray-scale and rotation invariant texture classification with local binary patterns," *Pattern Analysis and Machine Intelligence, IEEE Transactions on*, Vol. 24(7), pp. 971-987, 2002.
- [10] Ainslie, Michael A., and James G. McColm. "A simplified formula for viscous and chemical absorption in sea water," *The Journal of the Acoustical Society of America*, Vol. 103, pp. 1671, 1998.
- [11] Oja, E., and Kuusela, M. "The ALSM algorithm—an improved subspace method of classification," *Pattern Recognition*, Vol. 16(4), pp. 421-427, 1983.



Yasuhiro Tan

Yasuhiro Tan received the M.E degree in engineering from Kyushu Institute of Technology in 2003. He is presently studying Ph.D. course in Control Engineering in Kyushu Institute of Technology, Japan. His present research interests include the image processing, computer vision. He is a member of SICE and JASNAOE.

2010 and 2013. His research interests include three-dimensional shape/motion recovery, and human detection and its motion analysis from car videos. He is a member of IEEE, The Society of Instrument and Control Engineers, The Institute of Electronics, Information and Communication Engineers, and The Institute of Image Electronics Engineers of Japan.



Joo Kooi TAN

Joo Kooi TAN received the Ph.D degree in Control Engineering from Kyushu Institute of Technology. She is presently with Department of Mechanical and Control Engineering in the same university as Associate Professor. Her current research interests include three-dimensional shape/motion recovery, human motion analysis, and human activities recognition.

She received the SICE Kyushu Branch Young Author's Award in 1999, the AROB10th Young Author's Award in 2004, Young Author's Award from IPSJ of Kyushu Branch in 2004 and BMFSA Excellent Paper Award in 2008, 2010, and 2013. She is a member of IEEE, The Society of Instrument and Control Engineers, and The Information Processing Society of Japan.



Seiji Ishikawa

Seiji Ishikawa obtained B.E., M.E., and D.E. from The University of Tokyo, where he majored in Mathematical Engineering and Instrumentation Physics. He joined Kyushu Institute of Technology and he is currently Professor of Department of Control & Mechanical Engineering, KIT. Professor Ishikawa was a visiting research fellow at Sheffield University, U.K., from 1983 to 1984, and a visiting professor at Utrecht University, The Netherlands, in 1996. He was awarded BMFSA Excellent Paper Award in 2008,